

In the domain of metallurgy and ceramics, the properties of technological interest depend on the defect properties and on the defect structure of the material at the atomic (vacancies, impurities,...) or at the mesoscopic (dislocations, porosities, ...) level. This is why materials science requires a fundamental corpus of knowledge on defects and disorder. In particular, the fundamental study of atomically disordered systems allows to develop theoretical models, and to validate numerical simulations (Monte-Carlo, molecular dynamics, etc...) which are then applied to understand and modelize "real materials". Particularly important is the extrapolation of their properties at long time in operating conditions, and the prediction of their behaviour under thermal, chemical, or irradiation-induced ageing.

1. DISORDERED SYSTEMS

1.1. Introduction

The scientific activity of LLB in the field of disordered systems is mainly concentrated on the study of local atomic arrangements in topologically or chemically disordered solids or liquids, by elastic diffuse neutron scattering. Two instruments are entirely devoted to these studies :

- the 7C2 diffractometer, installed on the "hot" source, with short wavelength (generally $\approx 0.7 \text{ \AA}$) neutrons, and equipped with a 640 cell position sensitive linear multidetector, for liquid and amorphous systems,
- the G4.4 diffractometer, installed on a "cold" neutron guide, managed by ONERA and CEA/LSI, with time-of-flight analysis, devoted to the "in situ" high temperature study of local order in single crystals.

In the case of systems presenting a tendency towards phase separation, complementary studies by Small-Angle Neutron Scattering (SANS) are necessary.

Some studies of dynamics, mainly on glass transition, are also performed at LLB by external users, in particular with the time-of-flight inelastic spectrometer MIBEMOL.

1.2. Metallic alloys : from diffuse scattering to kinetics

(X. Flament, PhD, and R. Caudron, LLB and LEM-ONERA).

The face-centered cubic (f.c.c.) lattice contains equilateral triangles of first neighbours. If the interactions between these first neighbours dominate and are repulsive (antiferromagnetic), this results in a localized frustration. This frustration induces a degeneracy which is source of disorder and entropy, even at zero temperature. This phenomenon is at the origin of the complexity and of the richness of phase diagrams of systems built on the f.c.c. cubic lattice.

As shown by the diffuse neutron scattering study on Pd_3V , most of the order-disorder properties of this alloy, the structure DO_{22} of which is built on a f.c.c. cubic lattice, can be deduced from an Ising model limited to two interactions. In this model, the interactions J_2 between second neighbours are of the same sign, but much weaker than those between first neighbours J_1 ($J_2/J_1 \sim 0.05$). The work described here has allowed to show that, in this situation, the quasi-degeneracy presented by the DO_{22} phase can induce special ordering paths.

The Long-Range Order DO_{22} is characterised by 100 and $1 \frac{1}{2} 0$ type superstructure reflections. We have followed by X-ray diffraction the time dependence of the intensities of these two lines after in situ quenching. In the usual situations, one expects that, depending if the quench temperature is above or below the spinodal temperature, the two waves present, or not, an incubation time. In our case, two distinct spinodals exist, one for each concentration wave. If the quenching temperature is lower, or larger than the two spinodals, the two waves will increase instantaneously or not. This is what was found experimentally. Nevertheless, if the quenching temperature is intermediate, the wave with the lowest spinodal temperature will form instantaneously, while the other will undergo an incubation time. Figure 1a shows indeed that, for a quench from 660°C , the $1 \frac{1}{2} 0$ wave forms with a delay, when the 100 which, in the disordered state, corresponds to the maximum of short-range order intensity, develops immediately. On Fig.1b, a Monte-Carlo simulation reproduces clearly this situation, with J_1 and J_2 potentials compatible with the diffuse scattering determined by neutron scattering on G4.4.

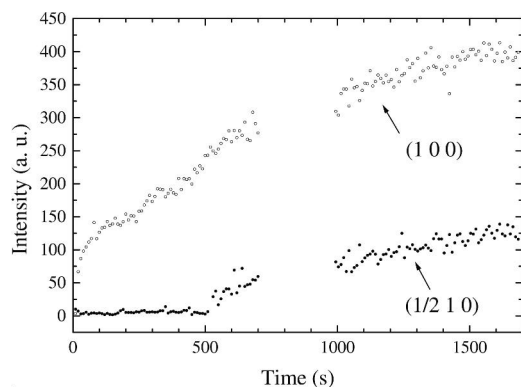


Figure 1a : Time evolution of the 210 (type 100) and 1 5/2 0 (type 1 1/2 0) Bragg peak maximum intensities following quenching from 660°C, determined by X-ray scattering (experiment performed at Brookhaven National Laboratory Synchrotron)

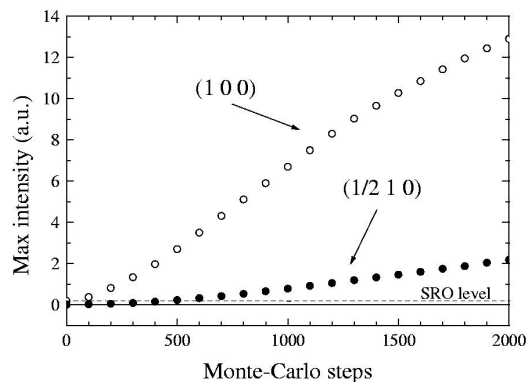


Figure 1b : Monte Carlo simulation of the results shown in Fig.1a . The dotted line shows the short-range order intensity in 100, confirming that the LRO concentration wave shows up instantaneously .

1.3. Short range order and phason fluctuations in icosahedral AlPdMn

(N. Shramchenko, PhD, R. Bellissent, LLB, D. Gratias and R. Caudron, LEM-ONERA)

The powder diffraction diagrams of quasicrystals were rapidly indexed after their discovery in 1984. This indexing was confirmed on single grains as soon as they became available. However, the exact location of the sites and their atomic occupancy are not yet known. The best models available nowadays concern only 90% of the sites.

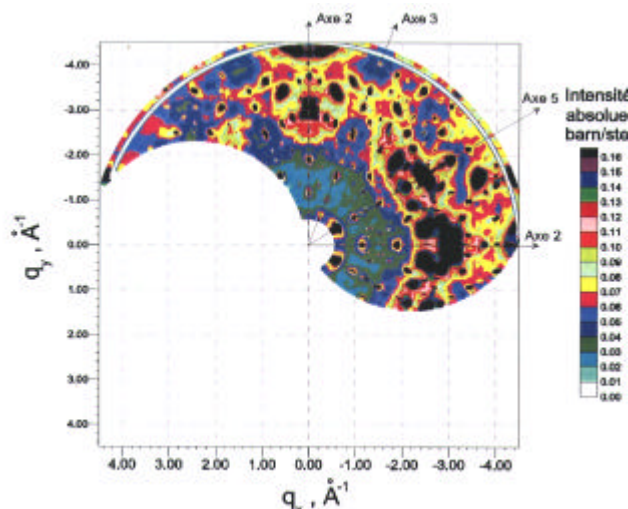
Diffuse scattering can provide us with information about partial occupancy of sites. We have studied at least four single crystals of AlPdMn icosahedral phase, elaborated by different teams, by Bridgeman or Czochralsky methods, and submitted to various heat treatments. All these crystals yielded, quantitatively, the same distribution of diffuse scattering. This situation can be attributed to the narrow domain of existence of the icosahedral phase (less than 3 at.%), and also to a low sensitivity of the diffuse scattering to the concentration and thermal treatment.

As an example, fig.2 shows this distribution in a two-fold symmetry plane containing two two-fold, two three-fold and two five-fold axes. The latter axes are indicated on the figure 2.

Spots corresponding to Bragg peaks are strongly broadened. This is not exactly peak broadening, but, in fact, a well identified diffuse scattering, due to phason fluctuations. We checked that this diffuse scattering varies as the inverse square of the distance to the peak. It should also be proportional to the effective quench temperature, but we did not detect any change from sample to sample, notwithstanding the various heat treatments of the samples.

Far away from any obvious Bragg peak (gray-green zone on fig.2) we estimated the order of magnitude of the diffuse background to 0.03 barn/steradian. Unless it results from the superimposition of the diffuse feet coming from the neighbouring Bragg peaks, it can be attributed to chemical disorder. The partial site occupancy found on the approximant phase ξ' corresponds to 0.01 barn/steradian.

Figure 2. Elastic diffuse scattering map of the "mono-quasi-crystal" ($\text{Al}_{0.704}\text{Pd}_{0.214}\text{Mn}_{0.082}$) measured at LLB on G4.4 at room temperature



1.4. Structure and Dynamics of Supercritical Water

(M.C. Bellissent-Funel, P. Calmettes, LLB, M. Bonetti, CEA/SPEC)

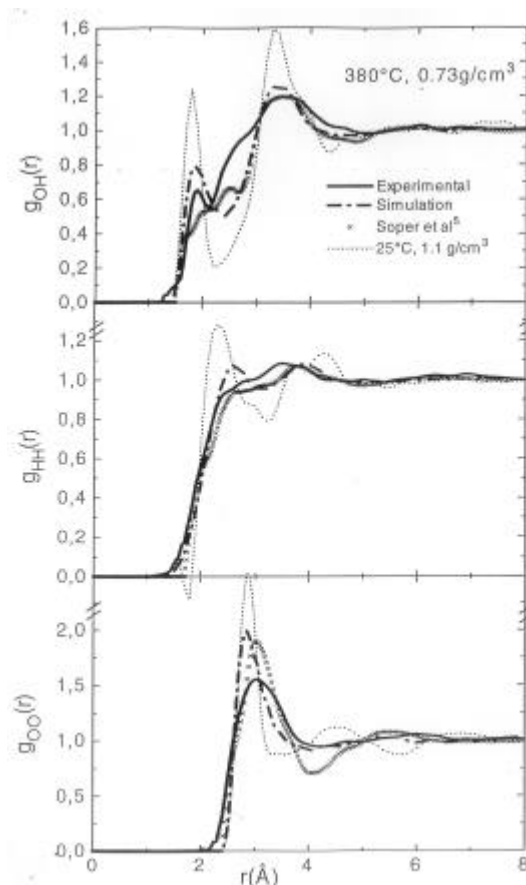
Liquid water has been studied extensively near ambient conditions. Much less is known about water under extreme conditions. Beyond the critical point (H_2O : $T_c \sim 374^\circ\text{C}$, $P_c \sim 221$ bar, $\rho_c \sim 0.32$ g.cm⁻³ and D_2O : $T_c \sim 371^\circ\text{C}$, $P_c \sim 220$ bar, $\rho_c \sim 0.36$ g.cm⁻³), water exhibits many peculiar properties such as the variation of dielectric constant, viscosity, ion product as a function of the density. Supercritical water is a very reactive medium that is very well adapted in many industrial applications.

Small-angle neutron scattering (SANS) measurements were performed on supercritical water to understand its peculiar behavior. This technique can probe length scales from the correlation length of the critical density fluctuations to the intermolecular distances. SANS spectra were recorded along the critical isochore at temperatures between ($T_c + 0.48$ K) and ($T_c + 22.02$ K). At the lowest values of the wave vector transfer q , the scattered intensity shows a pronounced increase due to the divergence of density fluctuations at the critical point. In the studied q range, from 0.07 \AA^{-1} to 0.34 \AA^{-1} , all the spectra can be accurately described by the Fisher-Langer correlation function provided that a multiplicative additional term describing both the molecular structure and the local order are taken into account. The value found for the amplitude of the critical correlation length is $x_0 = (1.36 \pm 0.05) \text{ \AA}$. This was the first measurement of x_0 for water.

The microscopic structure of supercritical water has been studied by neutron scattering at different thermodynamic states, for densities ranging from 0.2 to 0.7 g.cm⁻³. The experimental partial pair correlation functions $g_{\text{OH}}(r)$, $g_{\text{HH}}(r)$ and $g_{\text{OO}}(r)$ are compared with the results of molecular dynamics simulations using the (SPCE) model potential for water (see figure 3). The tetrahedral arrangement is lost but hydrogen bonding persists in dense supercritical water via the presence of dimers. This is revealed by the proton density of states that exhibits strong differences with that of ambient water, and is in good agreement with data obtained by NMR and Raman spectroscopies.

Hydrogen-bond dynamics of supercritical water has been investigated for the same thermodynamic states by quasi-elastic neutron scattering. The results have been analysed using a jump diffusion model; τ_0 , the residence time and D , the translational diffusion coefficient have been determined as a function of the density of supercritical water. Values of D are in very good agreement with those measured by NMR and increase strongly as the density of the medium decreases. The residence time τ_0 slightly increases as the density of supercritical water decreases, with a value ten times shorter than that measured in ambient liquid water (1ps). The whole results confirm that some degree of hydrogen bonding is present in dense supercritical water even though the tetrahedral coordination number leading to an extended network at room temperature is lost

Figure 3. The experimental and simulated partial pair correlation functions g_{OH} , g_{HH} and g_{OO} of supercritical water at $T=380^\circ\text{C}$ and $\rho=0.73\text{g/cm}^3$. The data of Soper *et al.* J. Chem. Phys., 106 (1997) 313-322, have been reported for comparison together with that for ambient liquid water.



Disordered Systems and Materials Science

1.5. Dynamics of ^4He confined in porous media at very low temperatures

(F. Albergamo, PhD, LLB)

The measurements of helium adsorption isotherms (at temperatures as low as 1.2 K) have been made possible by building up a suitable equipment at the laboratory; by this technique, a number of porous samples (Vycor glass, Geltech silica and MCM-41 powders) have been characterised. Subsequent inelastic neutron scattering measurements on MIBEMOL spectrometer (at $T = 1.2$ K) on ^4He confined into the 32 Å MCM-41 pores at different pore fillings have revealed that the bulk-like response (elementary excitations) comes from the ^4He in the capillary condensate phase.

Further investigation has been conducted on the same system at very low temperatures (down to 0.4 K) with the IN6 spectrometer at the ILL. Special sample cells, filled and sealed at room temperature, have been developed in order to avoid the use of the injection capillary on the ^3He cryostat that was found to allow condensation of unknown amounts of liquid helium. In this way, the thermodynamic state of the system was kept known through the whole experiment. For the first time, evidences for phonon confinement phenomena have been collected. In particular, a perturbation of the long wavelength phonon dispersion (up to $q = 0.55 \text{ \AA}^{-1}$) was observed. Further theoretical developments are in progress to account for this anomalous behaviour.

2. MATERIALS SCIENCE

2.1 Introduction

Materials Science aims to understand the properties of solid systems in their full complexity, and to optimize these properties by acting on the composition, atomic structure, and microstructure. This is a different approach to that of condensed matter physics, which focuses on model systems to study a given property or phenomenon. Obviously, materials science has an immediate bearing on industry and applications.

Neutrons are an ideal probe for studying the structure of materials, particularly because of their low absorption, which makes it possible to work on centimetre-thick parts, and the relative ease with which experiments can be carried out under complex or extreme conditions, such as high temperatures or applied stress.

Research currently under way at LLB includes studies on :

- Residual stress evaluation in complex systems,
- Evolution of textures with thermal or mechanical processing,
- Structure heterogeneity, precipitation, ageing of materials,
- Properties of coated glasses and gratings.

Studies on industrial materials are usefully complemented by studies of model materials that are easier to interpret. Methods for analysing the reciprocal lattice (neutron and X-ray scattering) and the real lattice (electron microscopy, atomic probe, near-field microscopy) are complementary, and always used together, especially for complex industrial materials.

2.2 Engineering - Residual stresses

(M. Ceretti, LLB; A. Lodini, University of Reims Champagne-Ardenne)

Residual stresses in materials have a considerable effect on material properties, including fatigue resistance, fracture toughness and strength. Neutron Strain Scanning provides a powerful non-destructive tool for stress analysis deep within a crystalline material. The principle of the technique is to use crystal lattice as an atomic strain gauge to measure strain distributions with a sub-millimetre spatial resolution. The stresses are thus calculated from the measured strains using elasticity laws. The main research activities developed in the last years at the LLB in this field can be summarised as follows:

- measurement of bulk stress in engineering components,
- understanding deformation processes in technological relevant materials,
- peak broadening analysis,
- development of a strain dedicated diffractometer, "DIANE" (G5.2) (in coll. With INFM, Italy).

Engineering activity at the LLB has strongly developed in the last two years. A large number of real industrial problems have been studied in collaboration with academic (see "Highlight" by M. Grosse et al) and industrial partners, or through European programmes (TRAINSS).

Among the principal industrial contracts we had last year, we mention the works carried out in collaboration with MAN Technologie AG (influence of thermal treatments on the residual stress evolution in ARIANE tank), with Aerospatiale (residual stresses in a welding between aluminium alloy plates for Airbus) and with SNECMA. The latter is described in more detail below.

New aeroengines design requires innovative materials offering high performances in term of lightness, stiffness and strength. At present SNECMA Moteurs studies the possibility to replace the traditional titanium alloy rotor bladed disc with Ti/SiC composite reinforced rotor bling (bladed ring), offering an improved strength-to-weight ratio. A prototype structure is shown in Fig. 4a. However, thermal residual stresses caused by the differences in thermal expansion coefficient between the two phases could have important consequences during the service life of the component. Neutron diffraction technique is the only tool to determine residual stresses non-destructively in depth. Moreover, as the technique is phase selective, it provides information for each phase of the composite separately. A set of experiments has been performed on the G52 strain diffractometer of the LLB, in order to analyse the stress evolution on a single component before (as fabricated) and after fatigue loading. For example, figure 4b reports the evolution of the phase stresses in the hoop direction for the as-fabricated bling. As it might be expected, large compressive hoop stresses are observed in the SiC fibres (-1000 MPa), together with lower tensile hoop stresses in the Ti alloy matrix (+500 MPa).



Figure 4a: The prototype Ti/SiC bling

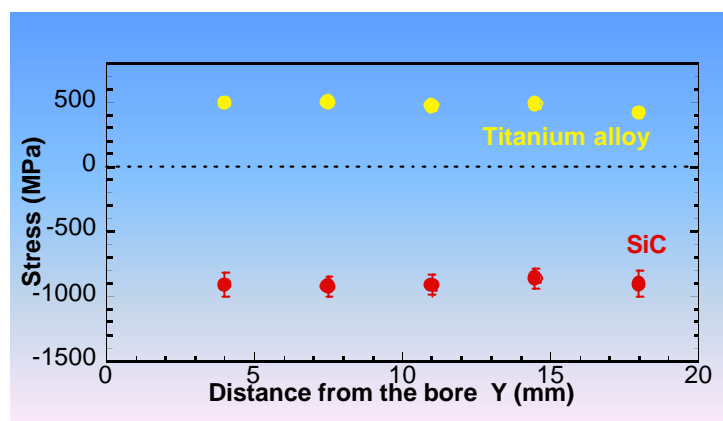


Figure 4b: Evolution of the hoop phase stresses as a function of the distance of the bore of the bling

In collaboration with the Czech team of Prague a spread activity on G52 is dedicated to peak broadening analysis to extract microstructural parameters from the measured profiles. The used approach includes both the influence of microstrain and size of coherently diffracting blocks as well as the instrumental resolution corrections. Modelling is performed in the reciprocal space and the microstrain contribution is treated according to the simple de Keijser's approach.

Recent studies in this field have been carried out to characterise stresses generated by shape memory alloy (P. Sittner, P. Lukas) and Nickel base superalloy (P. Lukas, J. Zrnik). In the latter case, the good instrumental resolution ($\Delta d/d \leq 2 \times 10^{-3}$) of the G52 diffractometer allows to distinguish the two overlapping peaks from γ' and γ phases, obtaining information on microstrains in matrix and precipitates.

Experiments over the last years have shown a varied research programme with stress analysis in a variety of materials from metals to rocks.

In the field of geology, the residual elastic strains determination by neutron diffraction has been performed on quartzite samples from a former texture study. The measured complete residual strain tensor has been considered as representative of the "natural" finite plastic deformation. Such tensors fitted to plastic tensors have been introduced in texture modeling, based on a self-consistent model. A good agreement between the experimental and the simulated results has been observed. This work was done in collaboration with the University of Cergy Pontoise and the LMS of Orsay University.

TRAINSS is a 4-year (1998-2001) european network, of the Brite-Euram III programme, involving neutron sources, Universities and industrials, aimed to train european industrial laboratories to the use of neutron

Disordered Systems and Materials Science

diffraction for determination of internal stresses. Two weeks per year of neutron beam time on the DIANE diffractometer are devoted to this programme to study specific problems brought by industrials, in our case SNCF and PSA-Peugeot-Citroen. The PSA problem is the determination of residual stresses in the discs of motor-car brakes, in order to define quality control criteria and to optimize the lifetime of the disks. SNCF is interested in the influence of residual stresses on the propagation of cracks in the wheel axles of railway engines and carriages sollicitated by oligocyclic fatigue in rotative flexion.

VAMAS TWA 20 is an international programme, the aim of which is to establish accurate and reliable procedures for making reproducible and standardized non-destructive neutron diffraction residual stress measurements. It includes representatives from industry, universities and 13 worldwide neutron sources. Different types of samples, in which residual stresses have been introduced by various procedures, are examined, according to a common protocol ("round-robin" testing). LLB has contributed significantly to this programme in the case of surface treatments (nickel alloy peened sample); the application of a software developed in collaboration with ENSAM, allowed to correct the systematic errors induced by close-surface effects, and to evaluate correctly the residual stresses as close as 25 μm from the surface.

The VAMAS programme is now finished; it will be followed by an European network entitled CEN/TC 138/AHG 7 : "NDT (Non Destructive Testing) - Residual stress measurement by neutron diffraction".

2.3 Textures

(M.H. Mathon, V. Branger, LLB; A. Baudin, A.L. Etter, LPCES, Orsay University)

Crystallographic texture (preferred orientation of grains) is one of the parameters describing the microstructure of a polycrystalline material. In metallic alloys, the texture appears during the solidification, then transforms during rolling or wire-drawing, and ultimately during recrystallization. The understanding and the mastering of its texture during thermomechanical and/or annealing treatments are necessary in order to optimise the mechanical behaviour of a material.

Neutron diffraction is the best technique for obtaining precise texture of bulk specimens ($\approx 1 \text{ cm}^3$), under the form of a distribution function of crystalline orientations. Its use is in particular necessary in the case of coarse-grained materials (\sim a few mm^3), where conventional X-rays are inapplicable.

LLB has a diffractometer specially devoted to the determination of crystallographic textures : 6Tl, equipped with an Euler cradle.

These last years, an important part of the texture activity has been dedicated to the study of recrystallization phenomena and to the evaluation of the stored energy. Indeed, during cold-work of a metal, a small fraction of the energy of deformation is stored in the crystal in the form of the elastic energy associated with the strain field of the generated dislocations. Grains of different crystallographic orientations are expected to store different amounts of energy during deformation. Since the stored energy is the driving force for recrystallization, its orientation dependence can influence the development of recrystallization texture components. The neutron peak broadening method was developed at the LLB to evaluate the stored energy as a function of the crystallographic orientations and it was applied to the FeNi alloys study.

The Fe53%-Ni alloy is widely used as soft magnetic sheet material. After high reduction (80%), this alloy exhibits copper-type cold-rolled texture with three main components : $\{110\}\langle 112 \rangle$ (B), $\{123\}\langle 634 \rangle$ (S) and $\{112\}\langle 111 \rangle$ (C). During recrystallization, a sharp cube texture $\{100\}\langle 001 \rangle$ appears, which is the case for fcc metals and alloys with medium or high stacking fault energy. On the other hand, for weaker cold-rolling, the recrystallization texture is similar to the rolling texture. The reason of this different behaviour is not clearly understood.

To study the kinetics of the recrystallization, we have performed "in-situ" isothermal texture measurements at the Risoe National Laboratory (Denmark) on the TAS3-TXTU spectrometer, equipped with a dedicated furnace. Figure 5a shows the kinetics evolution of S, B, C and cube components versus annealing time at 580°C. This reveals that the incubation time and the kinetics of the cube component development and of the deformation components disappearance are identical. These two phenomena seem to occur simultaneously, which proves that the recrystallization mechanism is not governed by oriented growth. Furthermore, the activation energy of the process involved during recrystallization, deduced from the evolution of the cube component (figure 5b), is equal to 2.5 eV, which is compatible with self-diffusion of fcc iron.

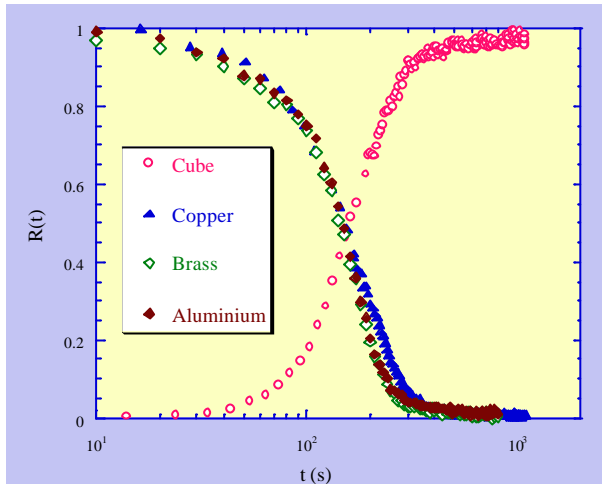


Figure 5a : S, B, C and cube components through the reaction advancement factor $R(t)$ (defined by $(I(t)-I(0))/(I(\infty)-I(0))$ with I the diffracted intensity), versus time during annealing at 580°C.

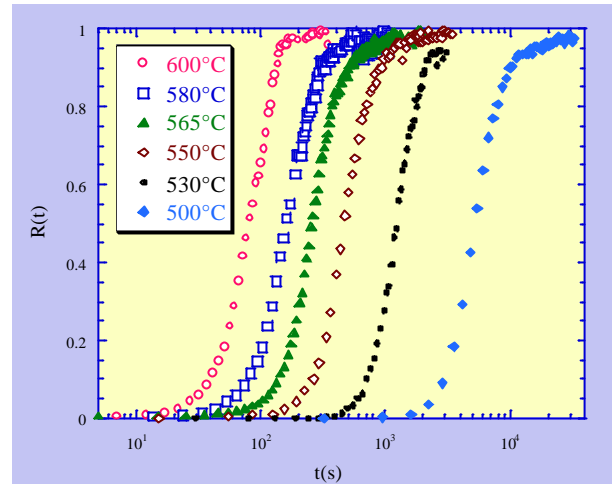


Figure 5b Cube component formation, through the reaction advancement factor $R(t)$, versus time for annealing temperatures between 500°C and 600°C.

To improve our understanding of the complex recrystallization mechanisms, the influence of the cold-rolled reduction on the stored energy was also studied. Low energy values are found for Cube grains present in a weak volume fraction after deformation whatever the reduction rate, and the energy gap between the Cube and the other texture components increases with reduction, promoting the Cube growth during recrystallization. For low reduction, no energy gap is observed and all orientations can grow simultaneously.

Furthermore, other fundamental and industrial studies have been performed at the LLB.

- A fundamental study of the deformation and recrystallization in a 50-50 austeno-ferritic steel has been undertaken in collaboration with the LPCES and the Institute of Metallurgy and Materials Science of Krakow (J. Jura). A surprising result is that the crystallographic texture of the b.c.c. α phase decreases, whereas that of the f.c.c. γ phase increases, with the deformation.
- A study of the relationships between the texture variation occurring during $\beta \rightarrow \alpha + \beta$ transformation and the microstructure has been performed on the high strength titanium alloy "BCEZ" developed for medium temperature compressor discs applications. This study has shown that whatever the microstructure, the texture components do not vary, but that their sharpness is sensitive to the morphology of the α phase. They were found to be insensitive to the intermediate ω phases, formed eventually during the precipitation sequence.
- Deformed quartz-rich rocks, which are rather ubiquitous in the upper part of the earth crust, show a wide range of microstructures and directional arrangements of the grains, producing a texture. Both the microstructures and crystallographic textures store informations about the deformation history of the host rock, which has recorded a complex strain path during its evolution, and therefore were used to supplement the macroscopic features of the deformation in rocks for the assessment of their kinematics. From samples collected in the Betic Cordillera (southern Spain), two principal components of the texture $\{\bar{1}2\bar{1}0\} < \bar{1}010 >$ and $\{\bar{1}10\bar{1}\} < \bar{1}\bar{1}20 >$ have been clearly identified and linked with specific proportions of grains considered respectively deformed and recrystallized. This work will now be completed by the study of annealed samples.

2.4. Nanomaterials prepared by mechanical alloying

(PhD thesis of S. Galdeano, coll. between M.H. Mathon, C.H. de Novion, LLB; L. Chaffron, CEA/SRMP; E. Vincent, CEA/SPEC; A. Traverse, LURE)

Mechanical alloying allows the synthesis of nanostructured materials, difficult or impossible to produce by classical routes, such as the $\text{Cu}_{80}(\text{Fe}_{0.3}\text{Co}_{0.7})_{20}$ compound which is constituted of a nanocrystalline Cu matrix in which are dispersed small $\text{Fe}_{0.3}\text{Co}_{0.7}$ clusters. The aim of this study is to precise the role of the milling

conditions on the nanostructure and on the spatial distribution of the magnetic atoms (Fe and Co), which influence the GMR properties of the material.

Batches of this ternary compound were produced by mechanical alloying elemental powders in a two-stage procedure involving first the preparation of binary $\text{Cu}_{88}\text{Fe}_{12}$ and $\text{Cu}_{72}\text{Co}_{28}$ f.c.c. metastable supersaturated solid solutions. At each stage of the preparation, the samples were characterised by X-ray and neutron powder diffraction, by SANS, by magnetic measurements, and by EXAFS.

These complementary techniques proved that in the ternary compound, the majority (60%) of the Fe and Co atoms are in form of superparamagnetic particles, either rich in Fe or mixed (Co+Fe). The rest is in a spin-glass type Cu-rich f.c.c. solid solution. The increase of the milling temperature (from 30 to 200°C) was shown to have important effects on the as-milled state : in particular the size of the magnetic clusters increases, and their internal structure changes from coherent f.c.c. to incoherent b.c.c. Fe-Co precipitates.

Further post-milling annealings, performed at 500°C, allow to enhance the precipitation of the magnetic particles. Even after a short annealing time (15 minutes), most of the superparamagnetic particles became ferromagnetic with a stoichiometry close to $\text{Fe}_{0.3}\text{Co}_{0.7}$. The increase of the milling temperature was clearly shown to slow down the post-milling precipitation kinetics, which is due to the change of the distribution of the superparamagnetic population (nuclei of the Fe-Co precipitates) with the milling conditions.

2.5. Structural stability of nuclear materials under thermal ageing or neutron irradiation

(M.H. Mathon, C.H. de Novion, LLB; Y. de Carlan, A. Alamo, CEA/SRMA; G. Geoffroy, B. Beuneu, A. Barbu, LSI, CEA/Ecole Polytechnique)

Since 1996, a research program is developed in the CEA on Low Activation Materials for nuclear applications. In order to characterise the microstructural evolution of martensitic steels under neutron irradiation (at 325°C up to a dose of 0.9 dpa), or after long thermal ageing (between 250°C and 550°C up to 22 000 hours), SANS experiments were coupled with Transmission Electron Microscopy (TEM) observations. They showed that above 8.8 at.% Cr in solid solution, the ferritic matrix is unstable at an ageing temperature of 400°C and separates into two b.c.c. phases, a Cr-depleted (α) and a Cr-rich (α'); moreover, a strong radiation-accelerated or induced α' precipitation is observed in alloys irradiated at 325°C. Finally, the precipitation of Laves phase $\text{Fe}_2(\text{Mo},\text{W})$ is strongly dependent on the Mo and W contents in the alloys.

Recently, SANS experiments allowed to check that the size and composition of oxide nanoparticles in different ODS (Oxide Dispersion Strengthened) steels, are stable after thermal treatments, which is a prerequisite for their selection as advanced fuel cladding for nuclear reactors.

2.6. Thin films and multilayers

(A. Menelle, F. Ott, P. Humbert (PhD), LLB, in coll. with C. Fermon, CEA/SPEC)

The major use of neutron reflectivity is in the field of magnetism (with polarised neutrons) and in soft matter. For non-magnetic and non-organic materials, X-ray reflectometry is the usual technique. Nevertheless, neutrons are useful in specific cases of poor X-ray contrast : e.g. layers of silicon oxide on silicon, or thin films containing titanium, which has a negative scattering length for neutrons.

This is the case of $\text{SiO}_y/\text{TiO}_x$ bilayers deposited on glass. Neutron reflectivity performed with Stazione Sperimentale del Vetro (Murano, Italy) provides better information than spectrophotometry and RBS on thickness, roughness and composition. The results have been used directly to calculate and optimise solar light and heat transmission properties of the coated glass.

The long lasting collaboration with Société CILAS on the development of Ti-Ni supermirrors is now going on through a more commercial basis. All technological research necessary before the product release in the market has been done. Now neutron reflectivity is used directly to check that the supermirrors produced by the company meets the specifications of the client.

More specialised are the efforts put in the study of non-specular reflectivity of periodic gratings. By comparison with experiments, we have validated a new program of non-specular intensity calculation. This opens the use of large gratings in instrumentation as a wavelength analysis device.

Another work on instrumentation has been our first surface diffraction experiment performed on the EROS reflectometer in order to demonstrate the efficiency of the new white beam method. It enables a fast and reliable alignment process, while the final diffraction measurements are performed using the usual time-of-flight method. Our main interest being in magnetic surface diffraction, the next experiment will be done using a polarised beam.